Delay-Robust Distributed Secondary Frequency Control: A Case Study

Sultan Alghamdi, Nathan Smith, Petros Aristidou
School of Electronic and Electrical Engineering
University of Leeds, Leeds, UK
{elsalg, el16njs, p.aristidou}@leeds.ac.uk

Johannes Schiffer
Institute of Electrical and Thermal Energy Systems
Brandenburg University of Technology, Cottbus, Germany
schiffer@b-tu.de

***Abstract*—With the purpose of enabling a low-carbon future, power systems worldwide are undergoing major transformations. These developments require new advanced control and operation approaches to ensure a stable and efficient system operation. Distributed consensus-based algorithms are a promising option to provide the necessary flexibility and scalability to cope with these challenges and have, thus, been widely investigated in the literature. Yet, most available results are limited to scenarios with reduced-order models and ideal communication. Motivated by this, we perform a case study using a detailed dynamic model of the well-known Nordic test system equipped with a consensus-based distributed secondary frequency controller. Our main objectives are to analyse the robustness of the closed-loop system with respect to unmodelled (voltage and higher-order generator) dynamics as well as communication delays. To facilitate the later property, we employ robust-stability conditions in the control design. Then, the performance of the proposed controller is assessed through detailed dynamic simulations covering several disturbances leading to large frequency and voltage excursions.**

***Index Terms*—Consensus algorithms, distributed control, secondary frequency control.**

I. Introduction

A. Motivation and Related Work

Power systems are seeing a growing demand to integrate more renewable energy sources (RES) for a more sustainable, low-carbon future. The rise in RES penetration means there is also an increase in power-electronic-interfaced components replacing conventional thermal generation units, hence reducing the total system inertia. This leads to new stability and security concerns involving frequency deviation and restoration, after a significant disturbance has occurred. Therefore, there is a need for advanced solutions through the use of new technologies and control approaches.

Regulating the steady-state frequency to the nominal value is required to maintain the balance between real-time generation and load. The latter is traditionally achieved by hierarchical control layers: primary, secondary and tertiary control [1]. The primary control is a proportional control that acts fast to stabilize the frequency in a decentralized fashion but cannot perform steady-state frequency restoration. Secondary frequency control adjusts the active power setpoints to compensate for the steady-state frequency deviation which results from the primary control operation and the disturbances.

The development of cyber-physical power systems comprising the combination of power systems and communication networks could promote new control techniques in this area and aid in reaching secondary frequency control goals by the utilisation of distributed communication architectures.

Conventionally, secondary frequency control is realized through a centralized scheme termed Automatic Generation Control (AGC), where the area control error is transmitted to the data center to be analyzed. Then new setpoints are broadcasted to each generator [2]. The resilience of future power systems is limited by the reliance of centralized approaches on a single control center; thus, making them vulnerable to single point failures.In addition, the need to minimise the complexity of communication infrastructures to achieve better scalability, makes centralized schemes inefficient. These challenges can be addressed with the use of new, distributed, schemes [3].

As a consequence, there is a need for transforming the power system from a centralized control scheme to a distributed architecture. To this end, much work has been dedicated to employing distributed control algorithms such as consensus approaches [4]–[6] and primal-dual gradient-based algorithms [7], [8] that incorporate both frequency restoration and optimal generator dispatch. The work in this paper considers consensus-based algorithms for secondary frequency control which rely on peer-to-peer communication where each generation unit exchanges information with neighbouring participating generators. In practice, the consensus-based controller is simpler to implement than the primal-dual algorithm and also does not require prior knowledge of the actual load demand nor the generator parameters and power flows. Furthermore, consensus-based control can guarantee an optimal steady-state resource allocation (with standard quadratic generation cost functions).

Employing communication networks in power system applications is however not problem-free and issues linked to communication time delays complicate the control design and may even deteriorate the system performance. In the case of the conventional AGC, delay robustness has been investigated in [9], [10] and in deregulated power systems in [11]. Delay-robustness of consensus-based secondary control schemes with respect to time-varying delays has been investigated for microgrids in [12] and for power systems in [13]. The latter work has been extended to generator models with higher-order turbine governor dynamics in [14] and these results are used for tuning the controllers in the present paper.

B. Contributions

Based on the above discussion, our paper provides for the first time an extensive case study that evaluates the performance of a consensus-based secondary frequency control scheme on a realistic, full-detailed, medium-scale power system under the explicit consideration of communication delays. Furthermore, it is empirically shown that the conditions for delay robustness established previously by part of the authors in [14] also could guarantee robust stability in the presence of additional unmodelled dynamics. Compared to the related work [6], [15], our case study is not only limited to verify the steady-state frequency restoration with economic dispatch but, in addition, explores the impact of communication delays as well as the interaction of the controller with unmodelled voltage phenomena. Our case study is performed on the Nordic test system [16] and simulated with the software RAMSES.

II. Optimal Consensus-Based Frequency Control

In this section, we present some essential background information on optimal resource allocation and delay-robustness of the employed consensus-based controller.

A. Reduced Power System Model

For the control development, we represent the power network using the Kron-reduction method [1] as a connected and undirected graph with set of nodes $\mathcal{N} = \{1, 2, \dots, n\}$. We assume that at each node a generator is connected and assign a phase angle $\theta_i : \mathbb{R}_{\geq 0} \to \mathbb{R}$ and a relative frequency $\omega_i = \dot{\theta}_i - \omega^d$, where $\omega^d \in \mathbb{R}_{\geq 0}$ is the desired (nominal) network frequency, to each unit $i \in \mathcal{N}$. It is convenient to define the vectors $\theta = \mathrm{col}(\theta_i)$ and $\omega = \mathrm{col}(\omega_i)$. Moreover, we make the following standard assumptions: the voltage amplitudes $V \in \mathbb{R}^n_{\geq 0}$ at all nodes are constant and the transmission line impedances are purely inductive [1]. With these assumptions, two nodes i and k are connected via a non-zero susceptance $B_{ik} \in \mathbb{R}_{<0}$. If there is no line between i and k, then $B_{ik} = 0$. We denote the set of neighboring nodes of node i by $\mathcal{N}_i = \{k \in \mathcal{N} | B_{ik} = 0\}$. The active power flow can be written as follows $P : \mathbb{R}^n \to \mathbb{R}^n$,

$$P(\theta) = \nabla U(\theta),$$

where the potential function $U : \mathbb{R}^n \to \mathbb{R}$ is given by

$$U(\theta) = - \sum_{\{i,k\} \in [\mathcal{N}]^2} |B_{ik}| V_i V_k \cos(\theta_{ik}).$$

Moreover, the electromechanical generator dynamics can be compactly written as

$$\begin{aligned} \dot{\theta} &= \omega, \\ M\dot{\omega} &= -D\omega - \nabla U(\theta) + P^{\text{net}} + P_m, \end{aligned} \tag{1}$$

where $P_m : \mathbb{R}_{\geq 0} \to \mathbb{R}^n$ is the mechanical power and $P^{\text{net}} = \mathrm{col}(P_i^d - G_{ii}V_i^2)$, where $P_i^d \in \mathbb{R}$ denotes the nominal power injection setpoint and $G_{ii}V_i^2$, $G_{ii} \in \mathbb{R}_{\geq 0}$, represents the active power demand at the i-th node. Furthermore, the diagonal and positive definite matrices $D \in \mathbb{R}^{n \times n}$ and $M \in \mathbb{R}^{n \times n}$ denote the damping and inertia coefficients, respectively.

Before introducing the turbine-governor dynamics as well as to motivate the need for a consensus-based secondary control law, we will study the steady-state frequency deviation of the system (1). Suppose that the solution of the system (1) converges to a synchronous motion with $\omega^s = \mathbb{1}_n \omega^*$, where ω^* is constant. Then, ω^* is obtained from

$$\mathbb{1}_n^\top M \dot{\omega}^s = 0 \quad \Rightarrow \quad \omega^* = \frac{\mathbb{1}_n^\top P^{\text{net}} + \mathbb{1}_n^\top P_m^s}{\mathbb{1}_n^\top D \mathbb{1}_n}, \tag{2}$$

where we have used the fact that $\mathbb{1}_n^\top \nabla U(\theta) = 0$. Clearly, in order to obtain a zero stationary frequency deviation, the total generated power needs to match the total consumption. In the present paper, we aim at achieving this classical secondary control objective by simultaneously allocating the stationary secondary control injections in an optimal fashion, i.e. by solving an economic dispatch problem online. Therefore, we introduce the following optimization problem [17]:

$$\begin{aligned} &\min_{P_m^s} \frac{1}{2} (P_m^s)^\top A P_m^s, \\ &\text{subject to } \mathbb{1}_n^\top P^{\text{net}} + \mathbb{1}_n^\top P_m^s = 0, \end{aligned} \tag{3}$$

where $A = \mathrm{diag}(A_{ii}) \in \mathbb{R}^{n \times n}$ is a diagonal positive definite weighting matrix. Hence, the cost function is quadratic and strictly convex. It can be seen from (2) that satisfying the constraint in (3) guarantees steady-state frequency restoration. The optimal solution to (3) is given by [4], [17], [18]

$$P_m^s = \alpha A^{-1} \mathbb{1}_n, \quad \alpha = \frac{\mathbb{1}_n^\top P^{\text{net}}}{\mathbb{1}_n^\top A^{-1} \mathbb{1}_n}. \tag{4}$$

Since P_m is the output of the turbine-governor system, we next introduce standard second-order turbine-governor dynamics together with a suitable distributed consensus-based secondary frequency controller, such that the stationary solutions P_m^s of the closed-loop power system correspond to optimal solutions of (3).

B. Turbine-Governor Dynamics

The speed of a synchronous generator is determined by the speed of the prime mover. One of the well-known prime movers is the steam turbine. The speed of the steam turbine is controlled by the speed governor that senses the speed deviation and converts it into an appropriate valve action [19]. It is common in stability analyses to use a simplified model for the steam turbine-governor model to facilitate the stability analysis such as the TGOV1 model, see [20]. In this paper, we use a modified version of the TGOV1 [19] together with a secondary frequency control signal which will be used to achieve steady-state frequency restoration.

The physical dynamics of the steam turbine-governor can be written as follows

$$\begin{aligned} T_m \dot{P}_m &= -P_m + P_s, \\ T_s \dot{P}_s &= -P_s - K^{-1}\omega + p, \end{aligned} \tag{5}$$

where $P_s : \mathbb{R}_{\geq 0} \to \mathbb{R}^n$ is the steam power and $p : \mathbb{R}_{\geq 0} \to \mathbb{R}^n$ is the secondary control signal. Furthermore, the diagonal and positive definite matrices $K \in \mathbb{R}^{n \times n}$, $T_m \in \mathbb{R}^{n \times n}$ and $T_s \in \mathbb{R}^{n \times n}$ denote the droop gains, governor time and turbine time constants, respectively.

C. Optimal Consensus-Based Frequency Control

Building upon [4], [14], we consider the following consensus-based secondary frequency control scheme for the

power system given by (1) and (5)

$$T_p\dot{p} = -p + P_m - (I_n - K^{-1})\omega - A\mathcal{L}Ap, \tag{6}$$

where the controller (6) is associated with an undirected connected communication network represented by the Laplacian matrix $\mathcal{L} \in \mathbb{R}^{n\times n}$ enabling distributed information exchange between the generators. The set of undirected edges of the communication graph is denoted by $\mathcal{E}$ and its cardinality by $|\mathcal{E}|$. Furthermore, the diagonal positive definite matrix $T_p \in \mathbb{R}^{n\times n}$ denotes the controller time constants. It has been shown in [4], [6], [17], that - if appropriately tuned - the control (6) is able to restore the frequency to its nominal value, that is, $\lim_{t\to\infty} \|\omega_i - \omega^d\| = 0$ for all $i \in \mathcal{N}$. In addition, it was shown in [6], [17] that in steady-state $P_m^s = p^s$ and that the power injections of all generation units satisfy the identical marginal cost requirement, i.e.,

$$A_{ii}P_{m,i}^s = A_{kk}P_{m,k}^s \quad \forall i \in \mathcal{N}, \quad \forall k \in \mathcal{N}. \tag{7}$$

Consequently, the matrix A is usually fixed by economic considerations and the stationary secondary control power injections correspond to optimal solutions of (3).

Guaranteeing robustness with respect to communication delays is essential for the implementation of (6) since delays pose a severe threat to the power system performance. Thus, we consider that the message sent from generation unit $i \in \mathcal{N}$ to generation unit $k \in \mathcal{N}$ over the m-th communication link is subjected to a constant communication delay $\tau_m > 0$.

In order to introduce the closed-loop system with communication delays compactly, we follow [13], [14] and introduce the matrices L_m, $m = 1, \ldots, 2|\mathcal{E}|$,

$$\mathcal{L} = \sum_{m=1}^{2|\mathcal{E}|} L_m. \tag{8}$$

Now, we define the vector $x = \text{col}(P_m, P_s, p) \in \mathbb{R}^{3n}$ as well as the matrices

$$T = \text{blkdiag}(T_m, T_s, T_p), \quad \bar{A} = \text{blkdiag}(A, A, A), \tag{9}$$

$$\Phi = \begin{bmatrix} I_n & -I_n & \mathbb{0} \\ \mathbb{0} & I_n & -I_n \\ -I_n & \mathbb{0} & I_n \end{bmatrix} \tag{10}$$

and

$$\Psi_m = \bar{A}\,\text{blkdiag}\left(\mathbb{0}, \mathbb{0}, L_m\right)\bar{A}. \tag{11}$$

Then, by combining (1), (5) with (6), the closed-loop dynamics with delays are given by

$$\begin{aligned} \dot{\theta} &= \omega, \\ M\dot{\omega} &= -D\omega - \nabla U(\theta) + P^{\text{net}} + \begin{bmatrix} I_n & \mathbb{0}_{n\times 2n} \end{bmatrix} x, \\ T\dot{x} &= -\Phi x - \left(\sum_{m=1}^{2|\mathcal{E}|} \Psi_m x(t-\tau_m)\right) - \begin{bmatrix} \mathbb{0} \\ K^{-1} \\ I_n - K^{-1} \end{bmatrix} \omega. \end{aligned} \tag{12}$$

As usual [12]–[14], we assume the following.

Assumption 1: The system (12) possesses an equilibrium point $\text{col}(\theta^s, \mathbb{0}_n, x^s) \in \mathbb{R}^{5n}$, such that

$$|\theta_i^s - \theta_k^s| < \frac{\pi}{2} \quad \forall i \in \mathcal{N},\ \forall k \in \mathcal{N}_i.$$

D. Delay-Robust Stability Condition

Following [13], [14], let $W \in \mathbb{R}^{3n\times 3n-1}$, such that $W^\top T^{\frac{1}{2}}\bar{A}^{-1}\mathbb{1}_{3n} = \mathbb{0}_{3n-1}$ and introduce the two matrices

$$\bar{\Phi} = W^\top T^{-\frac{1}{2}}\Phi T^{-\frac{1}{2}}W, \tag{13}$$

$$\bar{\Psi}_m = W^\top T^{-\frac{1}{2}}\Psi_m T^{-\frac{1}{2}}W. \tag{14}$$

We then employ the following result for designing the gains of the controller in (12), the proof of which is given in [14].

Proposition 1: Consider the system (12). Fix A, K, $\mathcal{L}$, T and D as well as $\tau_m \in \mathbb{R}_{>0}$. Suppose that for all Ψ_m defined in (11), there exist matrices $R_m > 0 \in \mathbb{R}^{(3n-1)\times(3n-1)}$, $S_m > 0 \in \mathbb{R}^{(3n-1)\times(3n-1)}$, $P > 0 \in \mathbb{R}^{(3n-1)\times(3n-1)}$, $P_2 \in \mathbb{R}^{(3n-1)\times(3n-1)}$, $P_3 > 0 \in \mathbb{R}^{(3n-1)\times(3n-1)}$ satisfying

$$\mathcal{Q} = \begin{bmatrix} -D & \mathcal{Q}_{12} & \mathcal{Q}_{13} & \mathbb{0}_{n\times(3n-1)} \\ * & \mathcal{Q}_{22} & \mathcal{Q}_{23} & \mathcal{Q}_{24} \\ * & * & \mathcal{Q}_{33} & \mathcal{Q}_{34} \\ * & * & * & -S-R \end{bmatrix} < 0, \tag{15}$$

where

$$\begin{aligned} &R = \text{blockdiag}(R_m), \qquad S = \text{blockdiag}(S_m), \\ &\mathcal{Q}_{12} = \frac{1}{2}\begin{bmatrix} I_n & \mathbb{0}_{n\times 2n} \end{bmatrix} T^{-\frac{1}{2}}W - \begin{bmatrix} \mathbb{0} & K^{-1} & I_n - K^{-1} \end{bmatrix} T^{-\frac{1}{2}}WP_2, \\ &\mathcal{Q}_{13} = -\begin{bmatrix} \mathbb{0} & K^{-1} & I_n - K^{-1} \end{bmatrix} T^{-\frac{1}{2}}WP_3, \\ &\mathcal{Q}_{22} = -P_2^\top\bar{\Phi} - \bar{\Phi}^\top P_2 + \sum_{k=1}^{2|\mathcal{E}|} S_k - \sum_{k=1}^{2|\mathcal{E}|} R_k, \\ &\mathcal{Q}_{23} = -\bar{\Phi}^\top P_3 + P - P_2^\top, \qquad \mathcal{Q}_{24} = \begin{bmatrix} \bar{\mathcal{Q}}_{24,1} \ldots \bar{\mathcal{Q}}_{24,2|\mathcal{E}|} \end{bmatrix}, \\ &\bar{\mathcal{Q}}_{24,m} = R_m - P_2^\top\bar{\Psi}_m, \qquad \mathcal{Q}_{33} = -P_3 - P_3^\top + \sum_{k=1}^{2|\mathcal{E}|} \tau_k^2 R_k, \\ &\mathcal{Q}_{34} = \begin{bmatrix} \bar{\mathcal{Q}}_{34,1} \ldots \bar{\mathcal{Q}}_{34,2|\mathcal{E}|} \end{bmatrix}, \qquad \bar{\mathcal{Q}}_{34,m} = -P_3^\top\bar{\Psi}_m. \end{aligned}$$

Then, the equilibrium point $\text{col}(\theta^s, \mathbb{0}_n, x^s) \in \mathbb{R}^{5n}$ is locally uniformly asymptotically stable (modulo rotational symmetry).

III. Test System and Results

In this paper, we use the well-known Nordic system [16], sketched in Fig. 1, to perform a case study, which consists of the following two scenarios. First, we test the effectiveness of the proposed delay-robust stability conditions in Proposition 1. This will be investigated by tripping a generator leading to a frequency deviation. This is depicted in Case 1. The second scenario, consisting of Case 2 and Case 3, has the main purpose of illustrating the interplay between the controller (6) and unmodelled voltage phenomena. The system is composed of three areas: the North, Central and South; with an equivalent external system connected to the North. It consists of 74 buses, 102 lines, 42 transformers (20 of them equipped with On-Load Tap Changers), and 20 synchronous generators (hydro in the North and thermal in the Central/South). The generators are represented by detailed dynamic synchronous machine models with excitation, power system stabilisers and governors. Finally, the distribution loads are represented with voltage-sensitive, restorative models. All the dynamic models are detailed in [16]. An $N-1$ *insecure* operating point is used to analyze the controller performance.

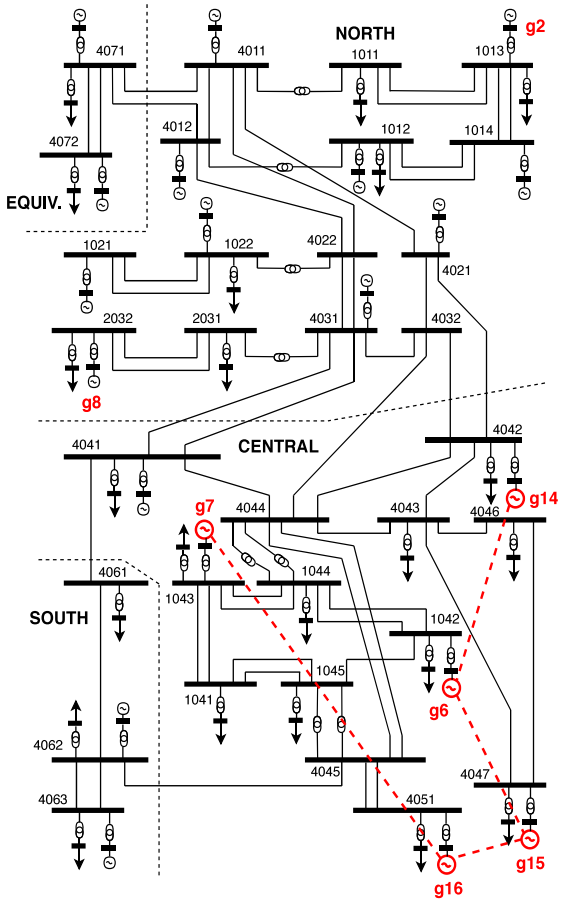

Fig. 1. Schematic representation of the Nordic test system taken from [16]

A. Implementation of Secondary Frequency Controller

In this section, we choose the gain of the distributed secondary frequency controller (6) for the described test system based on Section II. The distributed control is implemented at five of the thermal generators in the Central area (g6, g7, g14, g15, and g16) by replacing the constant mechanical power with the modified TGOV1 governor described by (5) and (6). The North area generators are equipped with hydraulic turbines.

For the communication network topology shown in Fig. 1 and for a maximum communication delay of 200 ms, we select the controller parameters T_p as follows. First, we form the matrix $\mathcal{L}$ in (6) based on the communication network topology and the matrix A in (6) based on the generator marginal costs. Then, we define $T_p = \frac{1}{0.04\kappa}A$, where 0.04 is the droop gain for the primary control, $\kappa \in \mathbb{R}_{>0}$ is a tuning parameter and we set the communication delay to the maximum allowed $\tau_m = \tau = 200$ms. Then, we select a large initial value of κ (that is, a small T_p and fast-acting controller) and decrease its value until the conditions (15) become feasible. This procedure gives us the fastest acting controller that satisfies the delay-robustness conditions. Moreover, this choice of T_P allows that generators with small cost coefficients (i.e., small A_{ii}) will react faster than the ones with large cost coefficients (i.e., large A_{ii}). Fig. 2 provides a feasibility map of the stability analysis conditions in (15) for the specific test system for different time delays and tuning parameter κ. The conditions are feasible in the shaded regions.

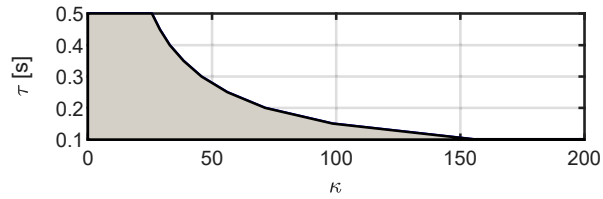

Fig. 2. The feasibility map of condition (15) with different maximum communication delays.

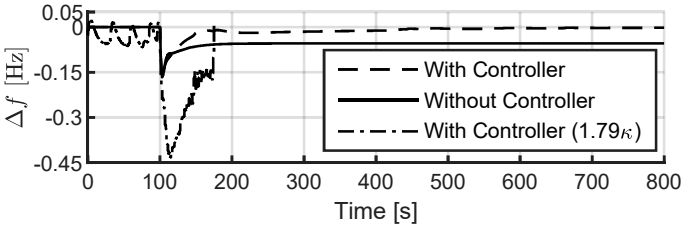

Fig. 3. Case 1: Frequency deviation

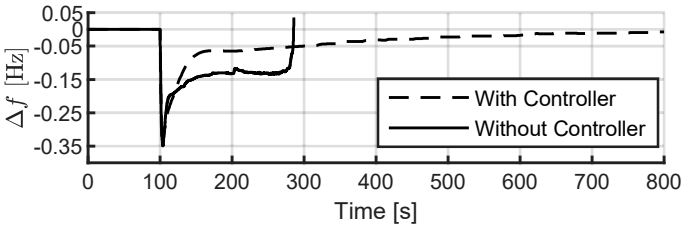

Fig. 4. Case 2: Frequency deviation

The feasibility of the analysis conditions (15) were implemented in MATLAB by using Yalmip [21] and Mosek [22] while all the dynamic simulations below were carried out using the simulation software RAMSES [23].

B. Case 1: Trip of 300MW Generator $g2$ in North Area

In this case, the 300MW thermal generator $g2$ is tripped at $t = 100$s in the North area resulting in a frequency deviation ($\Delta\omega$) that triggers the primary frequency response and the distributed secondary frequency controller. The frequency response is shown in Fig. 3, both with and without the proposed secondary frequency controller. We can see that in both variants the system is stable after the primary responses but in the second one, the proposed controller quickly restores the frequency to its nominal value, as desired. Furthermore, in order to investigate the conservativeness of the proposed condition in Proposition 1, we increase the value of κ, i.e. the response speed of the controller in RAMSES, while the value of the communication delays $\tau_m = \tau = 200$ms is fixed. We find that the performance of the system starts to significantly deteriorate from $\hat{\kappa} = 1.68\kappa$ until the system completely collapses at $\hat{\kappa} = 1.79\kappa$, see Fig. 3. We observe that the conditions in Proposition 1 are rather conservative for the considered scenario. Yet as discussed in [13], this may be explained by the fact that the conditions in Proposition 1 are equilibrium-independent and, hence, they are more conservative for equilibria with smaller phase angle differences (which is the case

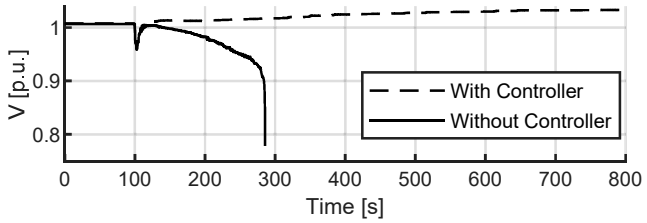

Fig. 5. Case 2: Bus voltage deviation at bus 1044 in Central area

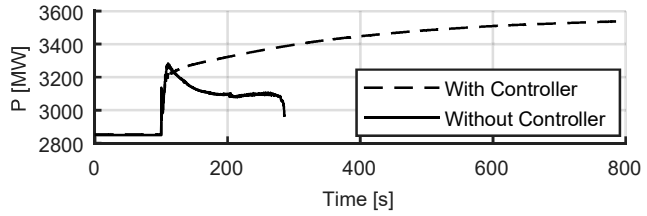

Fig. 6. Case 2: Total active power output from the participating generators

in the present scenario), but fairly accurate if the equilibrium phase angle differences are larger.

C. Case 2: Trip of 750MW Generator $g8$ in North Area

In this case, the large 750MW thermal generator $g8$ is tripped in the North area at $t = 100$s. Fig. 4 shows the frequency deviation both with and without the controller. It can be seen that without the secondary frequency controller the system collapses at $t \approx 240$s. The generation lost in the North causes depressed voltages in the Central area. As the voltages are restored (due to the combined effect of generator AVR and OLTCs actions), so is the load power consumption. The combined effect leads to a long-term voltage collapse [24], as shown in Fig. 5.

When the secondary frequency controller is used, the active power injected in the Central area as a response to the under-frequency deviation, stabilises the system and restores the frequency to its nominal value. This can be seen in Fig. 6 in which the total active power output of the generators participating in the secondary frequency control is shown.

Finally, Fig. 7 shows the controller exchanged variables reaching consensus in steady state after small deviations (see Fig. 7, zoom) right after the disturbance.

D. Case 3: Loss of Major Corridor Line

In the considered test system, active power is transferred from the North area (where most of the generation is located) to the Central area (where most of the load is located). In this case, we trip a branch located in the main corridor linking the Central and the North areas of the system, 4032-4044 in Fig. 1. This change limits the ability of the transmission system to evacuate power to the Central area.

First, this leads to a surplus of power in the North and a deficiency in the Central area. Consequently, we observe an initial over-frequency (see Fig. 8) accompanied with depressed voltages in the Central area (see Fig. 9). Later, the voltages in the Central area start being restored (along with the load power demand) and the frequency decreases below the nominal one.

This scenario leads to a long-term voltage collapse, driven by the load restoration and the generator over-excitation limits.

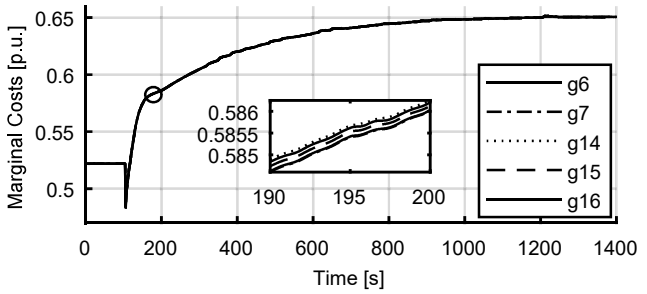

Fig. 7. Case 2: Convergence of controller outputs

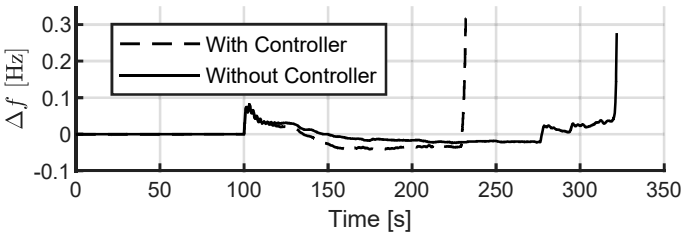

Fig. 8. Case 3: Frequency deviation

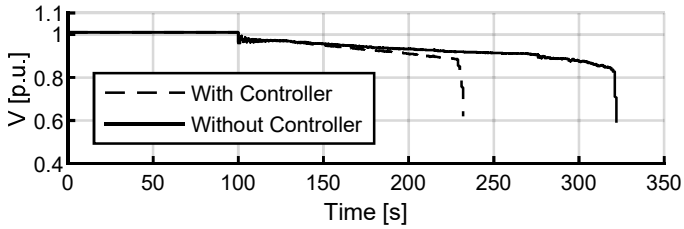

Fig. 9. Case 3: Bus voltage of bus 1044 in Central area

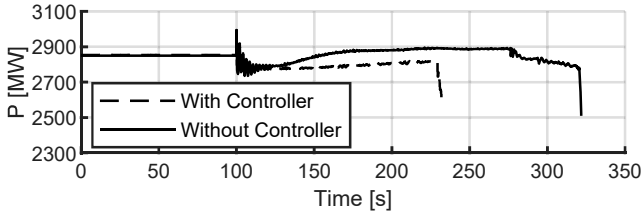

Fig. 10. Case 3: Total active power output from the participating generators

However, it can be seen from Figs. 8 and 9 that the proposed controller accelerates the system collapse.

The reasoning for the accelerated collapse is that the secondary controller reacts to the initial over-frequency by reducing the output power of the participating generators. Therefore, the power injected in the Central area is reduced, leading to a further reduction in bus voltages and accelerating the system collapse. Fig. 10 shows the total active power output of the generators participating in the secondary frequency control.

E. Discussion

The three cases above show the performance of the proposed controller under different operating conditions. In Case 1, a minor frequency problem is initiated due to the tripping of a generator. In this case, the dynamics are dominated by the generator and governor frequency response (1) and the behaviour of the controller is exemplar. Furthermore the delay-robust stability conditions derived in [14] and employed in the present work (see Proposition 1), have proven to be very

effective in this scenario, despite the presence of unmodelled system dynamics.

In Cases 2 and 3, the frequency dynamics initiated by the disturbance strongly interact with the long-term voltage dynamics driven by the load restoration mechanisms and the generator limits, leading to a complex dynamical interplay. This voltage-driven behaviour is not modelled in the controller analysis and, as the case study reveals, results in unforeseen system behaviours. In Case 2, the long-term voltage dynamics coincide with an under-frequency excursion, thus the controller response supports the system restoration by injecting more active power in the Central area. On the contrary, the behaviour of the controller in Case 3 leads to an accelerated system collapse due to the over-frequency excursion right after the disturbance that reduces the power injected in the Central area, thus further depressing the voltages.

Overall the presented case study analysis demonstrates that the proposed consensus-based secondary frequency control law (6) provides a flexible alternative to the standard AGC with the advantages of a fully distributed implementation and of combining frequency restoration with economic dispatch in real-time. The latter property may, e.g., also be used to enable peer-to-peer electricity markets [25].

But our investigations also show that the decoupling assumption between frequency and voltage dynamics, which is usually invoked when designing secondary frequency controllers [3], [4], [6], [7], [9], [14], can degrade the system performance in the presence of pronounced voltage dynamics following a disturbance. It is thus essential to be cautious when implementing the controller without considering such additional dynamics, in order to avoid deteriorating the overall system stability.

IV. Conclusions

We have investigated the performance of a consensus-based secondary frequency control via a case study on a detailed dynamic model of the Nordic test system. Two main aspects of interest were the robustness with respect to communication delays and with respect to unmodelled (voltage and higher-order generator) dynamics. Therefore, the controller has been designed by means of the delay-robust stability conditions derived in [14].

We have found that in the event of generator outages the steady-state frequency restoration was achieved in an optimal manner also in the presence of communication delays and unmodelled dynamics. Thus, the conditions in [14] were efficient. However, it was also shown that when complex voltage dynamics – not modelled in the control analysis phase – dominate the system behaviour, the controller might behave in an unexpected manner (stabilising or accelerating the system collapse).

Future work will therefore include the consideration of voltage dynamics, generator location and network topology in the analysis of the closed-loop performance to further improve the system resilience and robustness with respect to complex dynamic phenomena. Moreover, we will conduct a study to compare the performance of the proposed distributed controller with the standard centralized AGC under communication delays.

References

[1] P. Kundur, *Power system stability and control*. McGraw-Hill, 1994.

[2] J. Machowski, J. Bialek, J. R. Bumby, and J. Bumby, *Power system dynamics and stability*. John Wiley & Sons, 1997.

[3] C. Zhao, E. Mallada, S. H. Low, and J. Bialek, "Distributed plug-and-play optimal generator and load control for power system frequency regulation," *Int. J. Electr. Power Energy Syst.*, 2018.

[4] S. Trip and C. D. Persis, "Distributed optimal load frequency control with non-passive dynamics," *IEEE Trans. Control Netw. Syst.*, vol. PP, no. 99, pp. 1–1, 2017.

[5] J. Schiffer and F. Dörfler, "On stability of a distributed averaging PI frequency and active power controlled differential-algebraic power system model," in *ECC*. IEEE, 2016, pp. 1487–1492.

[6] A. Kasis, N. Monshizadeh, and I. Lestas, "A novel distributed secondary frequency control scheme for power networks with high order turbine governor dynamics," in *ECC*, 2018, pp. 2569 – 2574.

[7] T. Stegink, C. De Persis, and A. van der Schaft, "A unifying energy-based approach to stability of power grids with market dynamics," *IEEE Trans. Autom. Control*, vol. 62, no. 6, pp. 2612–2622, 2017.

[8] N. Li, C. Zhao, and L. Chen, "Connecting automatic generation control and economic dispatch from an optimization view," *IEEE Trans. Control Netw. Syst.*, vol. 3, no. 3, pp. 254–264, 2016.

[9] L. Jiang, W. Yao, Q. Wu, J. Wen, S. Cheng *et al.*, "Delay-dependent stability for load frequency control with constant and time-varying delays," *IEEE Trans. Power Syst.*, vol. 27, no. 2, p. 932, 2012.

[10] H. Bevrani and T. Hiyama, "A control strategy for LFC design with communication delays," in *IPEC*, 2005, pp. 1087–1092 Vol. 2.

[11] C. K. Zhang, L. Jiang, Q. H. Wu, Y. He, and M. Wu, "Delay-dependent robust load frequency control for time delay power systems," *IEEE Trans. Power Syst.*, vol. 28, no. 3, pp. 2192–2201, 2013.

[12] S. Alghamdi, J. Schiffer, and E. Fridman, "Distributed secondary frequency control design for microgrids: Trading off L_2-gain performance and communication efforts under time-varying delays," in *ECC*, 2018, pp. 758 – 763.

[13] J. Schiffer, F. Dörfler, and E. Fridman, "Robustness of distributed averaging control in power systems: Time delays & dynamic communication topology," *Automatica*, vol. 80, pp. 261–271, 2017.

[14] S. Alghamdi, J. Schiffer, and E. Fridman, "Conditions for delay-robust consensus-based frequency control in power systems with second-order turbine-governor dynamics," in *CDC*, 2018, pp. 786–793.

[15] C. Zhao, E. Mallada, S. H. Low, and J. Bialek, "Distributed plug-and-play optimal generator and load control for power system frequency regulation," *Int. J. Electr. Power Energy Syst.*, vol. 101, pp. 1 – 12, 2018.

[16] T. Van Cutsem, M. Glavic, W. Rosehart, J. Andrade dos Santos, C. Cañizares, M. Kanatas, L. Lima, F. Milano, L. Papangelis, R. Andrade Ramos *et al.*, "Test systems for voltage stability analysis and security assessment," IEEE, Tech. Rep., 2015.

[17] S. Trip, M. Bürger, and C. De Persis, "An internal model approach to (optimal) frequency regulation in power grids with time-varying voltages," *Automatica*, vol. 64, pp. 240–253, 2016.

[18] F. Dörfler, J. W. Simpson-Porco, and F. Bullo, "Breaking the hierarchy: Distributed control and economic optimality in microgrids," *IEEE Trans. Control Netw. Syst.*, vol. 3, no. 3, pp. 241–253, 2016.

[19] A. R. Bergen, *Power systems analysis*. Pearson Education India, 2009.

[20] P. Pourbeik *et al.*, "Dynamic models for turbine-governors in power system studies," *IEEE Task Force on Turbine-Governor Modeling*, 2013.

[21] J. Löfberg, "YALMIP : a toolbox for modeling and optimization in MATLAB," in *IEEE Int. Symposium on Computer Aided Control Systems Design*, Sept. 2004, pp. 284 –289.

[22] M. ApS, *The MOSEK optimization toolbox for MATLAB manual. Version 8.0.0.64*, 2017.

[23] P. Aristidou, D. Fabozzi, and T. Van Cutsem, "Dynamic simulation of large-scale power systems using a parallel schur-complement-based decomposition method," *IEEE Transactions on Parallel and Distributed Systems*, vol. 25, no. 10, pp. 2561–2570, 2014.

[24] T. Van Cutsem and C. Vournas, *Voltage Stability of Electric Power Systems*. Springer US, 1998.

[25] E. Sorin, L. Bobo, and P. Pinson, "Consensus-based approach to peer-to-peer electricity markets with product differentiation," *arXiv preprint arXiv:1804.03521*, 2018.